Article

High Catalytic Performance and Sustainability of Zr Modified Aluminophosphate for Vapor-Phase Selective *O*-Methylation of Catechol with Methanol

Xinfeng Ren, Dongfei Xu, Yuchen Yin, Xiujing Zou *, Yankai Wang, Xingfu Shang and Xueguang Wang *

State Key Laboratory of Advanced Special Steel, School of Materials Science and Engineering,
Shanghai University, Shanghai 200444, China; r1802773394@shu.edu.cn (X.R.); xudongfei@shu.edu.cn (D.X.);
ycyin@shu.edu.cn (Y.Y.); wangyankai@i.shu.edu.cn (Y.W.); xfshang@shu.edu.cn (X.S.)
* Correspondence: xjzou@shu.edu.cn (X.Z.); wxg228@shu.edu.cn (X.W.); Tel.: +86-21-66131615 (X.Z. & X.W.)

Abstract: Guaiacol produced by *O*-methylation of catechol with methanol over solid catalysts is a green environmental synthesis route. In order to achieve high catalytic efficiency, it is quite necessary to employ low-cost catalysts with high activity and stability. Herein, series of aluminophosphate catalysts were synthesized by a simple precipitation route modified by Zr. The characterization results indicated that the prepared Al-P-Zr catalysts possessed appropriate weak acid and weak base sites, which were beneficial for the *O*-methylation of catechol with methanol. Different Zr amount and calcined temperature exerted a significant influence on physicochemical properties of the catalysts and catalytic performance. The Al-P-Zr catalysts containing Zr/Al molar ratio of 0.012 calcined under 400 °C showed the optimal catalytic activity and long-term stability for vapor-phase selective *O*-methylation of catechol with methanol.

Keywords: catechol; *O*-methylation; Zr modified; aluminophosphate catalysts

1. Introduction

Guaiacol, also known as 2-Methoxyphenol, is an essential fine chemical intermediate, which is widely used in the synthesis of medicine, spices and dyes [1–3]. Due to the increasing attention of green chemistry and sustainable development, lots of endeavors are applied to exploit flexible catalytic process to synthesize guaiacol with eco-friendly reductant taking the place of poisonous and harmful agents [4–10]. Among the reported synthetic routes, vapor-phase *O*-methylation of catechol with methanol to produce guaiacol is receiving increasing attention because it is an economically and environmentally friendly route for industrial applications [6–10]. Except for the main product guaiacol, o-dimethyl ether is the main byproduct, and many further alkylation products are generated. The distribution of products (*O*-/*C*-methylation ratio) is mainly dependent on reaction parameters and physicochemical properties of the catalysts [7]. As a micro exothermic reaction, local overheating in the reaction process incline to produce carbon deposition and high carbon hydrocarbons [9]. Therefore, it is still a great challenge to develop a highly active and selective catalyst for vapor-phase *O*-methylation of catechol.

Several heterogeneous catalysts have been reported to be active in vapor-phase *O*-methylation of catechol and methanol, including pure and doped metal oxides [6–8], supported tungsten compound [9] and metal phosphates [10–16], etc. Amorphous aluminophosphates, which possess both acid and base sites, are considered effective catalysts for vapor-phase *O*-methylation of catechol with methanol [12–16]. The physicochemical properties of aluminophosphate have been reported to depend on modifying catalyst with various metals, optimizing catalyst compositions, and improving catalyst preparation routes [16–30]. Generally, aluminophosphates with specific structure are usually synthesized with various surfactant templates. However, it is difficult to adjust the acidic–basic

property for avoiding the structure destroyed [27–31]. Many synthetic methods, such as coated onto scaled zeolite [11], precipitation [12–14], citric acid route [15,16], etc., were widely used in preparation of aluminophosphates for vapor-phase *O*-methylation of catechol with methanol [18]. Nevertheless, most synthetic methods usually employ refluxed processing, additional ligand, and washing with distilled hot water, which leads to complex and/or high-cost preparation processes. Hence, it is still important to develop a simple approach to fabricate aluminophosphates with high activity and selectivity for vapor-phase *O*-methylation of catechol with methanol. It is commonly acknowledged that various metals, especially transition metal, introduced to aluminophosphates could alter the acid–base property of aluminophosphates [17–26].

In this paper, zirconium-aluminophosphates were prepared through a co-precipitation method with mixed metal nitrates with ammonium hydroxide. The effects of Zr content and calcined temperature on catalysts' physical and chemical properties were systematically investigated by XRD, N_2 adsorption, TPD, and IR. Their catalytic behavior for vapor-phase *O*-methylation of catechol with methanol was intensively investigated to design an effective catalyst for *O*-methylation.

2. Results and Discussion

2.1. Physicochemical Properties of $AlP_{1.1}Zr_x$-T

XRD patterns of the prepared samples are shown in Figure 1. The $AlP_{1.1}$-400 sample shows four weak diffraction peaks around $2\theta = 20.4°$, $21.7°$, $23.0°$, $35.7°$, corresponding to the reflections for $AlPO_4$ phase. Upon addition of Zr to $AlP_{1.1}$-400, the diffraction intensities of $AlPO_4$ phase disappear. Only a very broad band in the 2θ range of 15–30° corresponding to amorphous $AlPO_4$ [18,19,27] is observed on the $AlP_{1.1}Zr_x$-400 samples. These results demonstrate that the addition of Zr significantly promote the formation of smaller crystalline $AlPO_4$ particles. No characteristic diffraction peaks are observed associated with Zr species, likely due to highly dispersed Zr species with very small particle sizes below the detection limit of XRD measurements. As the calcined temperature increase from 350 °C to 500 °C, the XRD patterns of the samples in Figure 1b are not remarkably altered, revealing that the effect of calcination temperature on crystalline structure is negligible within the examined temperature range.
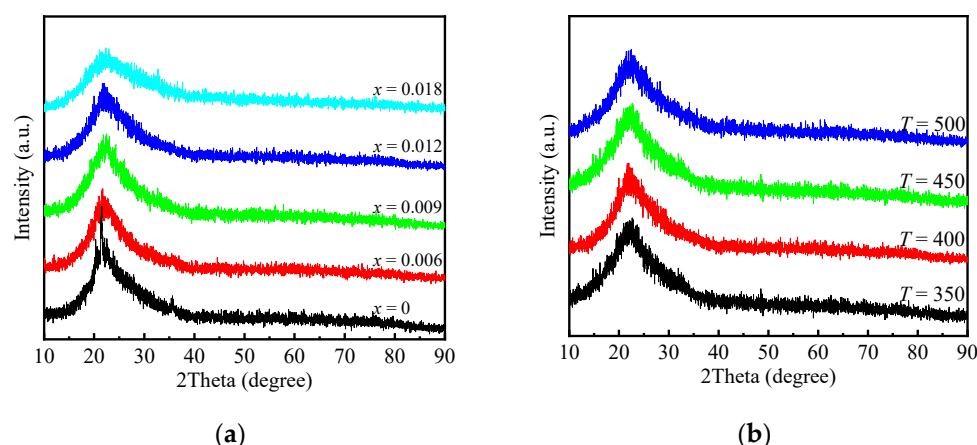

Figure 1. XRD patterns of the (**a**) $AlP_{1.1}Zr_x$-400 and (**b**) $AlP_{1.1}Zr_{0.012}$-T samples.

Figure 2 depicts the IR spectra of the prepared samples. The bands at 1134 and 495 cm^{-1} can be attributed to triply degenerate P-O stretching vibration and triply degenerate O-P-O bending vibration of tetrahedral PO_4^{3-}, respectively. The band at 726 cm^{-1}, assigned to the stretching vibration of Al-O in combination with P-O, begins to be weaken with the increasing Zr contents. This may be associated with the amorphous structure of $AlPO_4$ [17,18,27,31]. These results further indicate the structure of $AlPO_4$ of $AlP_{1.1}Zr_x$-T samples.

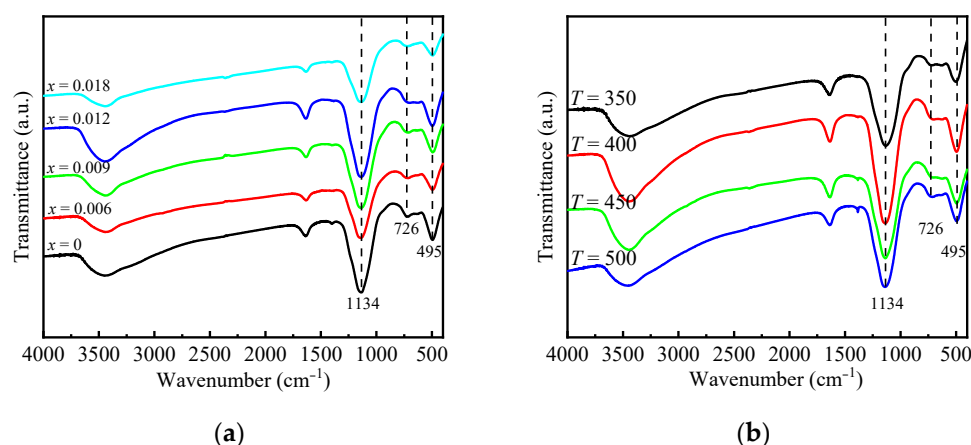**Figure 2.** IR spectra of (**a**) $AlP_{1.1}Zr_x$-400 and (**b**) $AlP_{1.1}Zr_{0.012}$-*T* samples.

The basic physical properties of the $AlP_{1.1}Zr_x$-*T* samples are summarized in Table 1. The $AlP_{1.1}$-400 had a specific surface area of 126 m^2/g, a pore volume of 0.83 cm$^3 \cdot$g^{-1}, and a pore size of 23.5 nm. The addition of Zr resulted in an increase of specific surface area and a decrease of pore size. There is a decreasing trend of the pore volume. However, the calcined temperature has no distinct difference on specific surface areas, pore volume, and BJH pore sizes. These results indicate that a certain amount of Zr can improve the S_{BET} of $AlP_{1.1}$ samples, likely due to the variation in the interaction between Al and P by Zr addition.

Table 1. Physical properties of $AlP_{1.1}Zr_x$-*T* catalysts.

Catalysts	S_{BET} (m^2 g^{-1})	V_p (cm$^3 \cdot$g^{-1})	D_a (nm)
$AlP_{1.1}$-400	126	0.83	23.5
$AlP_{1.1}Zr_{0.006}$-400	141	0.50	19.0
$AlP_{1.1}Zr_{0.009}$-400	163	0.84	17.2
$AlP_{1.1}Zr_{0.012}$-400	183	0.83	18.8
$AlP_{1.1}Zr_{0.018}$-400	195	0.68	15.0
$AlP_{1.1}Zr_{0.012}$-350	183	0.83	19.1
$AlP_{1.1}Zr_{0.012}$-450	181	0.82	18.8
$AlP_{1.1}Zr_{0.012}$-500	180	0.82	18.6

NH_3-TPD profiles are displayed in Figure 3. In terms of the $AlP_{1.1}$-400 sample, the NH_3-TPD profile illustrates two broad NH_3 desorption peaks centered at ca. 140 °C and 175 °C respectively, which are ascribed to two different weak acid centers [15]. In comparison with the $AlP_{1.1}$-400, the $AlP_{1.1}Zr_x$-400 samples show a dominant NH_3 desorption peak in the range of 80–250 °C, corresponding to unitary weak acid center [13]. The desorption peaks shift to higher NH_3 desorption temperature with the increasing Zr content, indicating that the addition of Zr strengthens the acidity of the catalysts. However, the area of the NH_3 desorption peak has no obvious change, likely due to adding a small quantity of Zr. These results indicate that the incorporation of Zr into the aluminum phosphate could alter the acidic strength without influencing the acidic amount of the samples. As for $AlP_{1.1}Zr_{0.012}$-*T* samples, the positions of desorption temperature shift to lower temperatures and the area of the desorption peaks in the range of 80–250 °C decrease with the elevating calcined temperature, meaning that increasing calcined temperature can decrease both the acidic strength and the acidic amount of the samples.
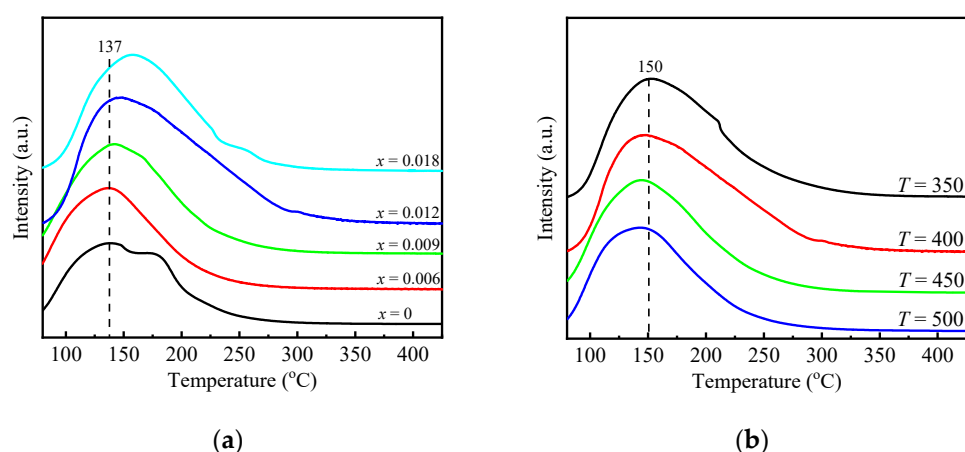
Figure 3. NH_3-TPD patterns of (**a**) $AlP_{1.1}Zr_x$-400 and (**b**) $AlP_{1.1}Zr_{0.012}$-T samples.

Figure 4 presents the Py-IR spectra of the $AlP_{1.1}Zr_x$-400 and $AlP_{1.1}Zr_{0.012}$-T samples. All the tested samples exhibit a weak band and two strong bands at 1542 cm^{-1}, 1492 cm^{-1}, and 1448 cm^{-1}, respectively. The weak band at 1542 cm^{-1} is attributed to the presence of trace amounts of Brönsted acidic sites. The strong band at 1448 cm^{-1} resulted from a great number of Lewis acidic sites. Notably, the strong absorbance at 1492 cm^{-1} is the co-adsorption of Brönsted and Lewis acidic sites [15,24,25]. By comparing with the NH_3-TPD results, we can deduce that all the prepared catalysts mainly possess weak Lewis acidic sites. Neither adding Zr to $AlP_{1.1}$-400 nor altering calcined temperature change the type of acid center.
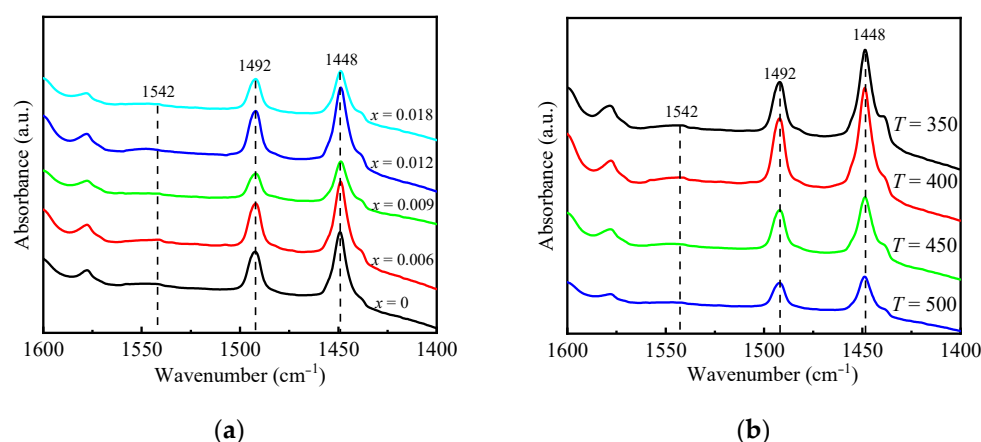

Figure 4. Py-IR spectra of (**a**) $AlP_{1.1}Zr_x$-400 and (**b**) $AlP_{1.1}Zr_{0.012}$-T samples.

CO_2-TPD was used to investigate the basic property of the prepared catalysts. Figure 5 displays the CO_2-TPD patterns of $AlP_{1.1}Zr_x$-T samples. The $AlP_{1.1}$-400 sample give a broad CO_2 desorption temperature peak centered at 170 °C, suggesting the presence of weak basic sites [15]. When a certain amount of Zr are added to $AlP_{1.1}$-400, the $AlP_{1.1}Zr_{0.006}$-400 sample displayed two broad CO_2 desorption peaks centered at 130 °C and 177 °C, respectively, with an appreciable decrease of the CO_2 desorption peak area. With increasing Zr content to x of 0.009, the CO_2 desorption peak centered 130 °C shift to a slightly lower temperature and the CO_2 desorption peak centered 177 °C shift to a higher temperature of ca. 210 °C. Meanwhile, the CO_2 desorption peak area decreased slightly. With further addition of Zr, no significant change occurs in the position and area of CO_2 desorption temperature on $AlP_{1.1}Zr_{0.012}$-400 and $AlP_{1.1}Zr_{0.018}$-400. The above results indicate that Zr addition increases the kinds of weak basic sites, alters the strength of basic sites, and decreases the number of base centers. With regard to the influence of calcination temperature on basic property, the patterns of CO_2-TPD is shown in Figure 5b. With the elevation of calcination

temperature, the CO_2 desorption peak centered at 130 °C shifts to higher CO_2 desorption temperature and the CO_2 desorption peak area decrease slightly, indicating that increasing calcined temperature can decrease the basic sites but increase the strength of basic sites of the samples.
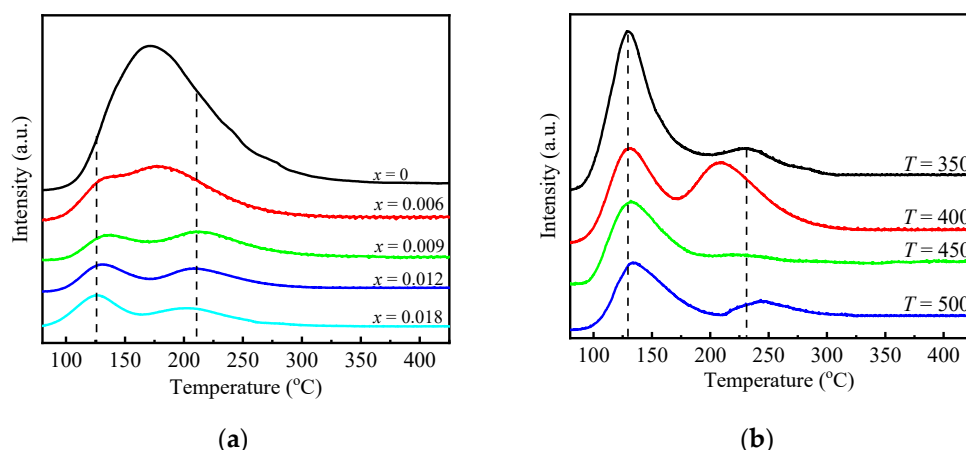

Figure 5. CO_2-TPD patterns of (**a**) $AlP_{1.1}Zr_x$-400 and (**b**) $AlP_{1.1}Zr_{0.012}$-T samples.

2.2. Catalysis Reaction

The catalytic performance of the prepared catalysts was investigated for vapor-phase selective *O*-methylation of catechol with methanol under optimized reactions. The effect of Zr content on catalytic performance is first investigated and the results are displayed in Figure 6. It can be seen that all the $AlP_{1.1}Zr_x$-400 catalysts exhibit high initial activities for the *O*-methylation of catechol. However, the catalyst stability obviously increases with increasing the Zr content in the range of 0.006–0.012. For example, the catechol conversion of $AlP_{1.1}Zr_{0.006}$-400 sample decline from 83% to 60% within the 12 h reaction time, while the catechol conversion is basically maintained at ca. 87% on the $AlP_{1.1}Zr_{0.012}$-400 sample. With the further increased Zr content, the $AlP_{1.1}Zr_{0.018}$-400 catalyst present poor stability for the *O*-methylation of catechol. After the reaction was carried out for 12 h, the catechol conversion decreased to 57%. Comparatively, $AlP_{1.1}$-400 shows an initial catechol conversion of 65% and 12 h catechol conversion of 54%. For all tested $AlP_{1.1}Zr_x$-400 catalysts, guaiacol selectivity is almost ca. 91%. The effect of calcination temperature on catalytic performance of the $AlP_{1.1}Zr_{0.012}$-T catalysts for selective *O*-methylation of catechol are provided in Figure 7. Catechol conversion increase with increasing calcination temperature from 350 to 400 °C. Further increasing the calcination temperature to 450 °C, the catechol conversion decrease. Guaiacol selectivity had a negligible effect on calcination temperature. The $AlP_{1.1}Zr_{0.0126}$-400 exhibited the optimal catalytic activity. Combined with the characterization of acid–base properties, the appropriate Lewis acidic sites and basic sites on $AlP_{1.1}Zr_{0.0126}$-400 contribute to the good catalytic performance for *O*-methylation of catechol, which is consistent with the reported in the literature [10,13].
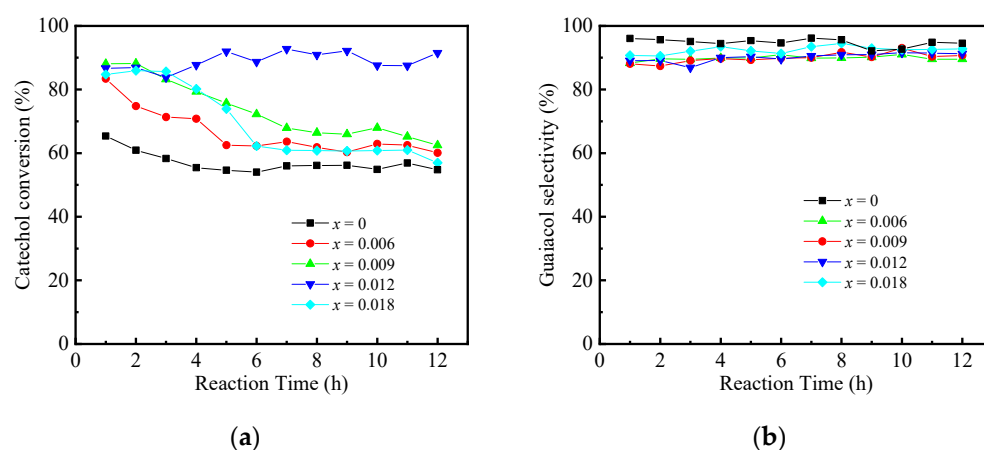
Figure 6. Catalytic performance of $AlP_{1.1}Zr_x$-400 catalysts. (**a**) catechol conversion; (**b**) guaiacol selectivity. Reaction condition: m_{cat} = 2 g, Reaction temperature = 553 K, LHSV = 0.2 h^{-1}, methanol/catechol = 5 (mol).

Figure 7. Catalytic performance of $AlP_{1.1}Zr_{0.012}$-T catalysts. (**a**) catechol conversion; (**b**) guaiacol selectivity. Reaction condition: m_{cat} = 2 g, Reaction temperature = 553 K, LHSV = 0.2 h^{-1}, methanol/catechol = 5 (mol).
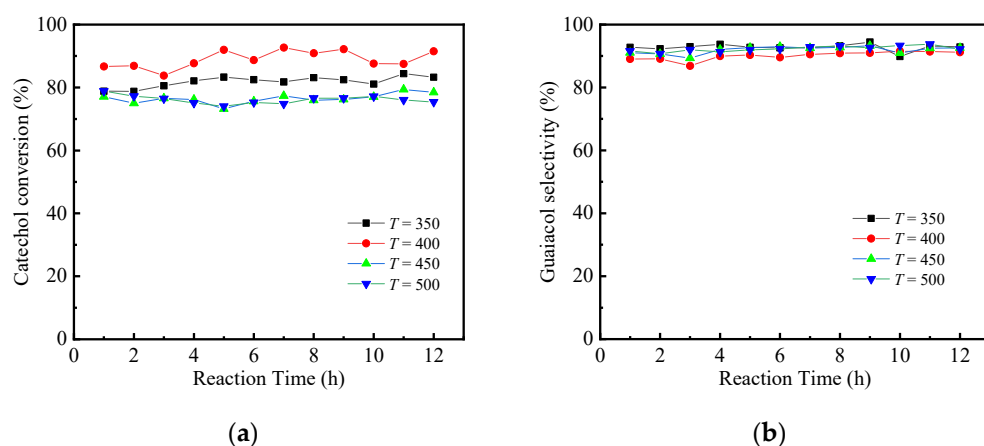
The stability tests were carried out for the selective *O*-methylation of catechol to guaiacol at 280 °C and LHSV = 0.2 h^{-1} with a methanol to catechol of 5 over $AlP_{1.1}Zr_{0.012}$-400 catalyst. One hundred–hour stability tests were conducted, and the results are shown in Figure 8. The initial catechol conversion and guaiacol selectivity are ca. 82.7% and 89.7%, respectively. Catechol conversion decrease slightly and guaiacol selectivity increase slightly in the initial reaction time of ca. 25 h, followed by the almost constant catechol conversion and guaiacol selectivity at ca. 80% and 92% respectively, during the subsequent 75 h reaction period. The $AlP_{1.1}Zr_{0.012}$-400 catalyst possess superior long-term stability for *O*-methylation of catechol. It has been established that carbon deposition is mainly responsible for the deactivation of acid/base catalysts. Thus, TG was employed to investigate the amount of carbon deposition on the spent $AlP_{1.1}Zr_{0.012}$-400 catalyst after 100 h of *O*-methylation of catechol (denoted as $AlP_{1.1}Zr_{0.012}$-400-S). For the $AlP_{1.1}Zr_{0.012}$-400-S, the deposited amount of carbon was only 44 mg/g$_{cat}$. These results demonstrated that the $AlP_{1.1}Zr_{0.012}$-400 catalyst possessed a stable coking resistance.

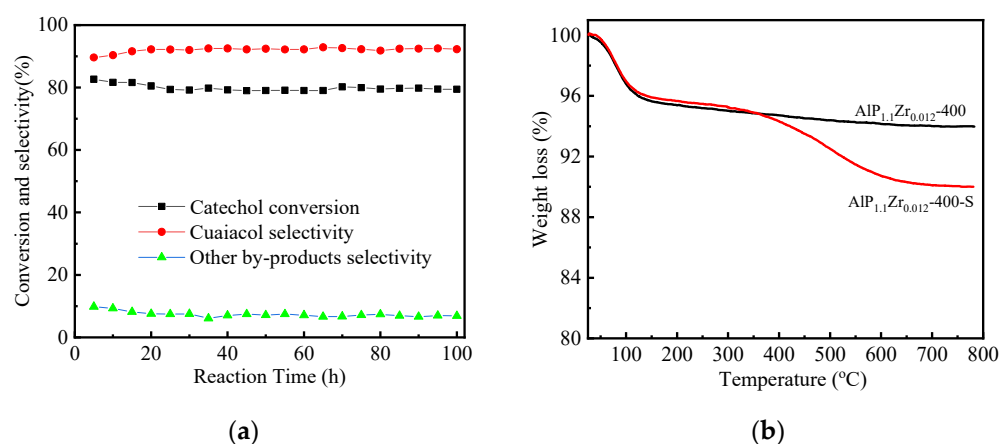**Figure 8.** (**a**) Catalytic properties as a function of time for the selective *O*-methylation of catechol over $AlP_{1.1}Zr_{0.012}$-400 catalysts. Reaction condition: m_{cat} = 2 g, Reaction temperature = 280 °C, LHSV = 0.2 h^{-1}, methanol/catechol = 5 (mol). (**b**) TG profiles of the $AlP_{1.1}Zr_{0.012}$-400 and $AlP_{1.1}Zr_{0.012}$-400-S catalysts.

3. Materials and Methods

3.1. Material Preparation

Zr modified aluminophosphate were prepared by a precipitation method, as noted previously [32]. A typical synthesis, stoichiometric aluminum nitrate, zirconium nitrate and ammonium dihydrogen phosphate were dissolved in 100 mL of deionized water. Then, a 28% ammonia solution was dropped into the mixed aqueous solution with vigorous magnetic stirring until the mixture completely precipitated. At this time, the pH value of the precipitate was ca. 10. Then, the obtained precipitate dried at 100 °C overnight. After that, the dried solid was calcined at a certain temperature for 5 h in air. According to the pre-experiment results, P/Al molar ratio is fixed at 1.1. The prepared materials were denoted as $AlP_{1.1}Zr_x$-*T*, where *x* represented Zr/Al molar ratio, and *T* represented the calcination temperature.

3.2. Material Characterization

XRD was performed with a D/Max-2550 diffractometer (Rigaku, Japan) using Cu K*a* radiation (40 kV, 200 mA). FT-IR spectra were recorded on a Tensor 27 spectrometer. Py-IR were acquired on a Nicolet iS50. Self-supporting wafers of pure catalysts were putted in the in-situ infrared cell, heated at 300 °C for 60 min, and then cooled to room temperature in vacuum of 10^{-4} mmHg. Pyridine was then exposed to the pre-treated samples at room temperature and was evacuated at 300 °C. BET surface areas of the catalysts were measured by N_2 adsorption–desorption using a Micromeritics ASAP 2020 Sorptometer (Micromeritics Instrument Corp., Norcross, GA, USA) at liquid nitrogen temperature (-196 °C). Before the measurement, each sample was degassed to eliminate volatile adsorbents on the surface at 300 °C for 6 h. TPD was carried out using NH_3 or CO_2 as probe molecules on homemade equipment to observe the acid and base properties of the catalysts. In a standard procedure, TPD measurements were carried out with 0.1 g of catalyst, placed in a quartz reactor and first pretreated in an Ar stream (40 mL min^{-1}) at 300 °C for 0.5 h to remove moisture and other absorbed impurities. The catalyst was cooled down to 50 °C and then exposed to a certain amount of ammonia or carbon dioxide for 0.5 h. After that, the system was swept with flowing Ar stream for 1 h. The catalyst was raised to 450 °C at a heating rate of 10 °C min^{-1} in Ar stream (40 mL min^{-1}). The amount of the desorbed NH_3 or CO_2 was measured with an online thermal conductivity detector. The identification of reaction products was analyzed with a gas chromatography-mass spectrometer (GC–MS) (Sunny Hengping Instrument, Shanghai, China). The column was an Agilent DB-5MS capillary column (cross-linked poly 5% diphenyl/95% dimethylsiloxane), 30 m $\times$ 0.25 mm (i.d.) $\times$ 0.25 μm film thickness. The oven temperature curve started at 130 °C and then rose

to 250 °C at a rate of 10 °C/min. The injection port and transfer line temperatures were both set at 250 °C. The ion source temperature was set at 230 °C. The amount of carbon deposition on the used samples was determined with a STA 4449 F3 thermogravimetric analyzer (Netzsch, Germany). The used catalysts were pre-treated at 50 °C for 30 min and then heated up to 800 °C with a rate of 10°C min^{-1} in an air flow of 30 mL min^{-1}.

3.3. Catalytic Test

The selective *O*-methylation of catechol to guaiacol was conducted in a vertical continuous-flow fixed-bed reactor (inner diameter of 8 mm and a length of 800 mm) at atmospheric pressure. Prior to the reaction, the catalyst (40–60 mesh) was first disposed in situ at 280 °C for 0.5 h in nitrogen. The reactant of the pre-mixed catechol–methanol mixture was controlled using a syringe pump. The products were analyzed with a gas chromatograph equipped with a capillary column and were identified using known standards and GC–MS.

4. Conclusions

AlP$_{1.1}$Zr$_x$-*T* catalysts were successfully prepared through a simple process of precipitation method without organic surfactants and used for selective *O*-methylation of catechol to guaiacol. AlPO$_4$ species, mainly in the form of smaller crystalline AlPO$_4$ particles, produced weak acidic and basic sites. Both Zr addition and calcination temperature had an influence on the strength and amount of the acidic and basic sites. AlP$_{1.1}$Zr$_{0.012}$-400 catalyst exhibited optimal catalytic properties with a superior guaiacol selectivity and catechol conversion. The stability test showed that AlP$_{1.1}$Zr$_{0.012}$-400 retained long-term stability without deterioration during the 100 h reaction period.

Author Contributions: X.R., D.X., Y.Y., and Y.W. performed the experiments and analyzed the data; X.S. contributed reagents/analysis tools; X.Z. wrote the paper; X.W. undertook project administration. All authors have read and agreed to the published version of the manuscript.

Conflicts of Interest: The authors declare no conflict of interest.

References

1. Llevot, A.; Grau, E.; Carlotti, S.; Grelier, S.; Cramail, H. From Lignin-derived Aromatic Compounds to Novel Biobased Polymers. *Macromol. Rapid Commun.* **2016**, *37*, 9–28. [CrossRef] [PubMed]
2. Mao, J.B.; Zhou, J.X.; Xia, Z.; Wang, Z.G.; Xu, Z.W.; Xu, W.J.; Yan, P.F.; Liu, K.R.; Guo, X.W.; Zhang, Z.C. Anatase TiO$_2$ activated by gold nanoparticles for selective hydrodeoxygenation of guaiacol to phenolics. *ACS Catal.* **2017**, *7*, 695–705. [CrossRef]
3. Kakhlon, O.; Ferreira, I.; Solmesky, L.; Weil, M.; Senderowitz, H.; Lossos, A.; Alvarez, R.; Pampou, S.; Escriba, P.; Yue, W. Guaiacol can be a drug-candidate for treating adult polyglucosan body disease. *Neurology* **2018**, *17*, e99694.
4. Lui, M.Y.; Lokare, K.S.; Hemming, E.; Stanley, J.N.G.; Perosa, A.; Selva, M.; Masters, A.F.; Maschmeyer, T. Microwave-assisted methylation of dihydroxybenzene derivatives with dimethyl carbonate. *RSC Adv.* **2016**, *6*, 58443–58451. [CrossRef]
5. Kabra, S.K.; Huuhtanen, M.; Keiski, R.L.; Yadav, G.D. Selectivity engineering of O-methylation of hydroxybenzenes with dimethyl carbonate using ionic liquid as catalyst. *React. Chem. Eng.* **2016**, *1*, 330–339. [CrossRef]
6. Vishwanathan, V.; Balakrishna, G.; Rajesh, B.; Jayasri, V.; Sikhwivhilu, L.M.; Coville, N.J. Alkylation of catechol with methanol to guaiacol over sulphate-modified zirconia solid acid catalysts. *React. Kinet. Catal. Lett.* **2007**, *92*, 311–317. [CrossRef]
7. Vishwanathan, V.; Balakrishna, G.; Rajesh, B.; Jayasri, V.; Sikhwivhilu, L.M.; Coville, N.J. Alkylation of catechol with methanol to give guaiacol over sulphate-modified zirconia solid acid catalysts: The influence of structural modification of zirconia on catalytic performance. *Catal. Commun.* **2008**, *9*, 2422–2427. [CrossRef]
8. Fu, Z.H.; Yu, Y.; Yin, D.L.; Xu, Y.Z.; Liu, H.P.; Liao, H.Y.; Xu, Q.; Tan, F.Q.; Wang, J. Vapor-phase highly selective *O*-methylation of catechol with methanol over ZnCl$_2$ modified-Al$_2$O$_3$ catalysts. *J. Mol. Catal. A Chem.* **2005**, *232*, 69–75. [CrossRef]
9. Zou, X.J.; Zhu, X.M.; Li, X.M.; Wang, Z.L.; Liu, G.; Jia, M.J.; Zhang, W.X. Vapour-phase *O*-methylation of catechol with methanol on SiO2-supported ammonium metatungstate catalysts. *Chin. J. Catal.* **2008**, *29*, 671–676.
10. Jafari, A.A.; Khodadadi, A.; Mortazavi, Y. Vapor-phase selective *O*-alkylation of catechol with methanol over lanthanum phosphate and its modified catalysts with Ti and Cs. *J. Mol. Catal. A Chem.* **2013**, *372*, 79–83. [CrossRef]

11.　Liao, X.Z.; Zhou, Z.; Wang, Z.L.; Zou, X.J.; Liu, G.; Jia, M.J.; Zhang, W.X. Preformed precursor of microporous aluminophosphate coating on mesoporous SBA-15: Synthesis, characterization, and catalytic property for selective *O*-methylation of catechol. *J. Colloid Interface Sci.* **2007**, *308*, 176–181. [CrossRef]

12.　Liu, G.; Yang, L.X.; Wu, S.J.; Jia, M.J.; Zhang, W.X. Influence of acid-base properties of K-loaded aluminophosphate catalysts on their catalytic behavior in the *O*-methylation of catechol. *Acta Phys. Chim. Sin.* **2014**, *30*, 1163–1168.

13.　Zhu, X.M.; Liu, X.M.; Jia, M.J.; Liu, G.; Zhang, W.X.; Jiang, D.Z. Vapour-phase selective *O*-methylation of catechol with methanol over Ti-containing aluminium phosphate catalysts. *Appl. Catal. A Gen.* **2005**, *282*, 155–161. [CrossRef]

14.　Mao, H.F.; Li, X.L.; Xu, F.; Xiao, Z.B.; Zhang, W.X.; Meng, T. Vapour-phase selective *O*-Methylation of catechol with methanol over metal phosphate catalysts. *Catalysts* **2021**, *11*, 531. [CrossRef]

15.　Liu, G.; Wang, Z.L.; Jia, M.J.; Zou, X.J.; Zhu, X.M.; Zhang, W.X.; Jiang, D.Z. Thermally stable amorphous mesoporous aluminophosphates with controllable P/Al ratio: Synthesis, characterization, and catalytic performance for selective *O*-methylation of catechol. *J. Phys. Chem. B* **2006**, *110*, 16953–16960. [CrossRef]

16.　Liu, G.; Jia, M.J.; Zhou, Z.; Zhang, W.X.; Wu, T.H.; Jiang, D.Z. Synthesis of amorphous mesoporous aluminophosphate materials with high thermal stability using a citric acid route. *Chem. Commun.* **2004**, *10*, 1660–1661. [CrossRef]

17.　Dai, W.L.; Kong, W.B.; Wu, G.J.; Li, N.; Li, L.D.; Guan, N.J. Catalytic dehydration of methanol to dimethyl ether over aluminophosphate and silico-aluminophosphate molecular sieves. *Catal. Commun.* **2011**, *12*, 535–538. [CrossRef]

18.　Wang, H.F.; Wang, Y.Y.; Liu, W.R.; Cai, H.H.; Lv, J.H.; Liu, J.D. Amorphous magnesium substituted mesoporous aluminophosphate: An acid-base sites synergistic catalysis for transesterification of diethyl carbonate and dimethyl carbonate in fixed-bed reactor. *Micropor. Mesopor. Mat.* **2020**, *292*, 109757. [CrossRef]

19.　Hamza, A.; Nagaraju, N. Amorphous metal-aluminophosphate catalysts for aldol condensation of n-heptanal and benzaldehyde to jasminaldehyde. *Chin. J. Catal.* **2015**, *36*, 209–215. [CrossRef]

20.　Sun, D.L.; Mai, J.J.; Deng, J.R.; Idem, R.; Liang, Z.W. One-Pot synthesis of dialkyl hexane-1,6-dicarbamate from 1,6-hexanediamine, urea, and alcohol over zinc-incorporated berlinite ($ZnAlPO_4$) catalyst. *Catalysts* **2016**, *6*, 28. [CrossRef]

21.　Luo, Y.S.; Liang, X.H.; Li, X.Q.; Wang, S.F.; Gao, X.N.; Zhang, Z.G.; Fang, Y.T. Iron doped aluminophosphate molecular sieve with improved adsorption capacity for water vapor. *Adsorption* **2018**, *24*, 551–561. [CrossRef]

22.　Vijayasankar, A.V.; Nagaraju, N. Preparation and characterisation of amorphous mesoporous aluminophosphate and metal aluminophosphate as an efficient heterogeneous catalyst for transesterification reaction. *Cr. Chim.* **2011**, *14*, 1109–1116. [CrossRef]

23.　Yan, X.; Qiu, Y.C.; Han, Y.D.; Sun, Q.M.; Ge, R.; Song, X.W. Microwave-assisted synthesis of a thermally stable Zn-containing aluminophosphate with ERI-zeotype structure templated by diquaternary alkylammonium. *RSC Adv.* **2014**, *4*, 49846–49849.

24.　Vijayasankar, A.V.; Deepa, S.; Venugopal, B.R.; Nagaraju, N. Amorphous mesoporous iron aluminophosphate catalyst for the synthesis of 1,5-benzodiazepines. *Chin. J. Catal.* **2010**, *31*, 1321–1327. [CrossRef]

25.　Kustov, L.M.; Kustov, A.L.; Kazansky, V.B. Spectroscopic investigation of redox and acidic properties of Co-substituted aluminophosphate CoAPO-11. *Mendeleev Commun.* **2018**, *28*, 354–356. [CrossRef]

26.　Kumar, A.; Sarmah, B.; Srivastava, R. C-N bond formation by the activation of alkenes and alkynes using Cu present in the framework and extra-framework of aluminophosphate. *Catal. Commun.* **2018**, *109*, 43–49. [CrossRef]

27.　Harish, N.; Kathyayini, N.; Nagaraju, N. Studies on the catalytic activity of mesoporous aluminaaluminophosphate (Al_2O_3–$AlPO_4$) materials in the synthesis of N.N′-diphenyl urea. *React. Kinet. Mech. Catal.* **2018**, *125*, 937–949. [CrossRef]

28.　Shyamprasad, K.; Shamshuddin, S.Z.M.; Shyamsundar, M.; Thimmaraju, N. Modified mesoporous aluminophosphate as an efficient solid acid catalyst for the synthesis of novel O- and N-acetylated compounds: Solvent free condition. *J. Porous Mat.* **2016**, *23*, 1095–1105. [CrossRef]

29.　Shi, J.H.; Liu, G.; Fan, Z.Q.; Nie, L.Y.; Zhang, Z.H.; Zhang, W.X.; Huo, Q.S.; Yan, W.F.; Jia, M.J. Amorphous mesoporous aluminophosphate as highly efficient heterogeneous catalysts for transesterification of diethyl carbonate with dimethyl carbonate. *Catal. Commun.* **2011**, *12*, 721–725. [CrossRef]

30.　Dawaymeh, F.; Elmutasim, O.; Gaber, D.; Gaber, S.; Reddy, K.S.K.; Basina, G.; Polychronopoulou, K.; Al Wahedi, Y.; Karanikolos, G.N. Metal substitution effects of aluminophosphate AlPO4-5 as solid acid catalyst for esterification of acetic acid with ethanol. *Mol. Catal.* **2021**, *501*, 111371. [CrossRef]

31.　Wang, J.C.; Liu, Q. Synthesis, characterization, and base–catalytic performance of ordered mesoporous aluminophosphate oxynitride materials. *J. Mater. Res.* **2007**, *22*, 3330–3337. [CrossRef]

32.　Akri, M.; El Kasmi, A.; Batiot-Dupeyrat, C.; Qiao, B.T. Highly active and carbon-resistant nickel single-atom catalysts for methane dry reforming. *Catalysts* **2020**, *10*, 630. [CrossRef]